Reduction of Current Harmonics in Data Center Power System using Single-Phase Shunt Active Power Filter

V. Zeleničić, M. Miletić, K. Raič Raguž, D. Sumina and I. Erceg
University of Zagreb/Faculty of Electrical Engineering and Computing
vinko.zelenicic@fer.hr, marinko.miletic@fer.hr, katica.raic-raguz@fer.hr, damir.sumina@fer.hr, igor.erceg@fer.hr

***Abstract*—With the significant increase of nonlinear loads in data center power systems, the losses due to the injection of current harmonics have also increased significantly. In order to reduce current harmonics, the use of Shunt Active Power Filters (SAPF) has become widespread. These filters use active components such as IGBT or MOSFET as well as R, L and C passive components. The SAPF power stage consists of a voltage source inverter (VSI) and an LCL filter, which is used to filter the signal at the switching frequency. The paper presents two simulatons of SAPF. The first simulation refers to a filter used only to reduce the current harmonics, while the second simulation uses a filter that also acts on the current reactive component. The control loop consists of a current controller and a PWM. In the first simulation, the grid side current and the converter side current are used as the current feedback signal. In the second simulation, only the grid side current is used as the current feedback signal. The results of two SAPF simulations are compared and the results show the influence of the control methods on the total current distortion as well as on the current ripple.**

***Keywords*—harmonic; active filter; voltage source inverters; reactive component**

I. INTRODUCTION

Recently, the need for data storage and processing has increased, and with it the need for data centres. Nonlinear loads in data centers, such as servers, IT equipment and cooling systems, are the most common sources of current harmonics. Harmonics not only increase the heating of equipment and shorten its life, but also have an impact on increasing overall losses in the system. The most common method for harmonic reduction is the use of active filters. Active filters compensate current harmonics by injecting equal but opposite harmonic compensating current. Type L and LCL filters are the most commonly used filters for reducing current harmonics. The LCL filter attenuates the high frequencies better than the L filter because the capacitor acts as a short circuit at high frequencies [1]. In addition, the LCL filter has a smaller volume for the same filtering effect and thus lower production costs. The LCL filter disadvantage is that they have current spikes at the resonant frequency [2]. It is necessary to provide damping at the resonant frequency to overcome this shortcoming. This attenuation can be passive or active. In the active method, fewer additional losses are introduced into the system, but the control loop is more complicated due to the additional control of active elements [3]. The passive damping method introduces additional losses into the system, but is the preferable option for more complex systems. In the simplest passive method, a resistor is connected in series with the capacitor. In contrast, in improved versions of passive methods, an inductor or a combination of inductor and capacitor is connected in parallel with the resistor. Due to their simplicity and good harmonic filtering characteristics, Shunt Active Power Filters with damping resistors have the widest application. This paper examines such a method.

In order to improve the properties of the LCL filter, the improved parameter design method of LCL SAPF is presented in [1]. In series with the capacitor, a resistor, an inductor, and a capacitor are connected in parallel. To design the inductor L_1 on the inverter side, which is used to suppress the inverter output current ripple, the peak ripple current method is used. For the best filtering effect, the two inductors ratio L_1/L_2 can be selected between 3 and 5. The filter's capacitance value (C_f) is designed to the systems rated power, and the reactive power generated by the capacitance is less than 5%. The damping inductor L_d short-circuits the damping resistor R_d at low frequencies, and the damping capacitor C_d short-circuits the resistor R_d at high frequencies. Conventional and improved LCL filters are compared in MATLAB/SIMULINK simulations, and the results show that the improved LCL filter has higher filter accuracy for higher harmonics.

A comparison of four different passive damping methods for LCL filter is given in [4]. Topologies, transfer functions and frequency characteristics are presented. Simulations for all methods were performed on an 80 kVA SAPF using the MATLAB/SIMULINK software package. Losses, damping efficiency, and performance were compared. The results show that the best attenuation of low frequencies up to resonance has the first method, where a resistor R is added in series with the capacitor of the LCL filter. Frequencies between the resonant and switching frequency are best attenuated by the second method, which involves connecting a parallel of the resistor and inductor in series with the capacitor. Frequencies above double switching frequency are best attenuated with third method which includes connecting a parallel resistor, an inductor, and a capacitor in series with the capacitor. Frequencies

This work has been fully supported by the European Regional Development Fund under the project "Development of a system for optimizing power consumption in data centers" (KK.01.2.1.02.0082).

approximately equal to the switching frequency are best attenuated by the fourth method, which adds a parallel of resistor and a series connection of inductor and capacitor in series with the capacitor. It is concluded that additional losses for all methods have a small effect on efficiency.

To improve the properties of the LCL filter the SAPF control system has two loops, the outer and the inner loop have feedback by grid current [5]. The inner loop is the PI control and the outer loop is the repetitive control, where the controller accumulates the error signal cycle by cycle and the error in this cycle occurs again in the next cycle. The PI control corrects the frequency characteristics and improves the dynamic response speed, while the repetitive control ensures the control system accuracy in a steady-state. A line voltage feedforward control has been used to suppress the influence of line fluctuations. The results show significant influence is in the low and medium frequency range. The voltage feedforward also reduces the line current *THD*. The experimental results show faster speed responses, good disturbance rejection, and higher accuracy in a steady-state compared to conventional SAPF control.

Another example of current control system is presented in [6]. In the LCL filter, there is no resistor in series with capacitor C. Resonance is prevented by an additional internal control loop. The internal circuit uses the capacitor current as a feedback signal. The coefficient (R) in the capacitor current feedback acts on the LCL filter attenuation like a physical resistor, which is why it is called a *virtual resistance*. The internal circuit stabilizes the control system, and the external circuit provides the required accuracy with a PI controller. Using the damping method with a virtual resistor improves the SAPF efficiency.

This paper compares the results of two Shunt Active Power Filters simulations when grid side and converter side currents are used as feedback signals. The paper is divided into four sections. Section I consists of an introduction and related work. In Section II, circuit and control diagrams of SAPF with LCL output filter are presented. Section III presents a comparison of the two simulations results. In the first simulation, measured values of the current harmonics were used, while in the second simulation the diode rectifier with an RL load on the DC side was used. Future work and conclusion are given in Section IV.

II. CONTROL MODELS

Fig. 1 shows the SAPF scheme with the LCL output filter. The grid side current (i_2) and the converter side current (i_1) can be used as the current feedback signal. To achieve the desired LCL damping factor resistor is connected in series with the capacitor. Transfer function, where ($L = L_1 \parallel L_2$) is given by (1). The resonant frequency of the second order term in the denominator is given by (2), and the damping factor ζ is given by (3).

$$G(s) = \frac{1}{s(L_1 + L_2)} \frac{RCs + 1}{LCs^2 + RCs + 1} \tag{1}$$

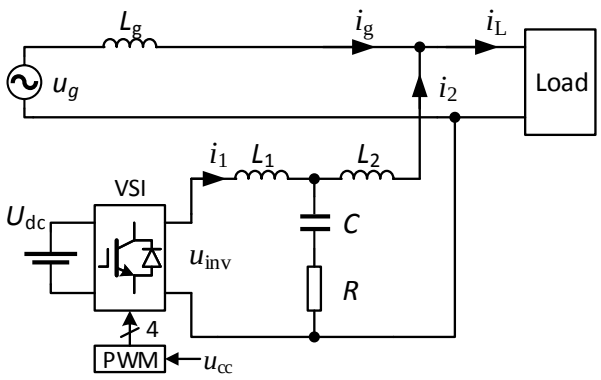

Fig. 1: Circuit diagram of SAPF with LCL output filter

$$\omega_n = \frac{1}{\sqrt{LC}} \tag{2}$$

$$\zeta = \frac{R}{2}\sqrt{\frac{C}{L}} \tag{3}$$

The inductance L_1 on the converter side has a value of 2 mH, the inductance L_2 on the grid side has a value of 0.5 mH and the capacitor has a value of 8 μF. The desired damping factor ζ is 1.41 and is achieved with a resistance value of 20 Ω.

The VSI consists of a single-phase transistor bridge with a constant DC voltage of 450 V. The transistors are controlled by a PWM circuit with a constant switching frequency of 16.7 kHz. Fig. 2 shows two different non-linear loads. Load 1 is a diode rectifier with RL load on the DC side, which is standardly used for obtaining current harmonics in experimental verification. When the RL circuit time constant is more than 30 ms (3 half cycles of the supply voltage), the RL circuit current pulsation is less than 7%, so that the current i_L on the AC side is almost rectangular. Such a waveform is rich in harmonics and is therefore suitable for SAPF experimental verification. The values for resistance and inductance are 13 Ω and 0.48 H, respectively. Load 2 is designed as a current source representing the actual current harmonics obtained by measurements in the data center. The current source consists of odd current harmonics up to the 25th harmonic.

Fig. 3 shows a control diagram of an APF filtering only the higher current harmonics, without compensation of the

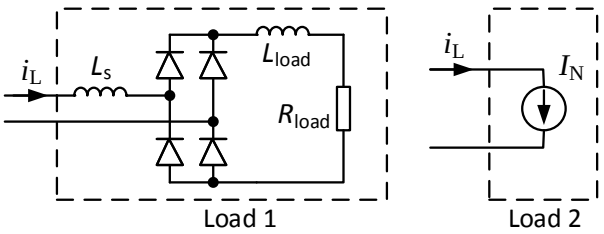

Fig. 2: Different SAPF Load

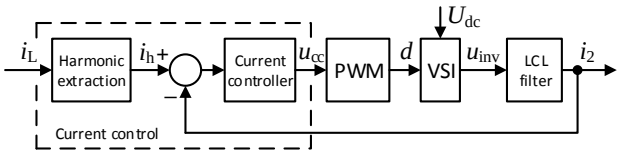

Fig. 3: SAPF Control diagram

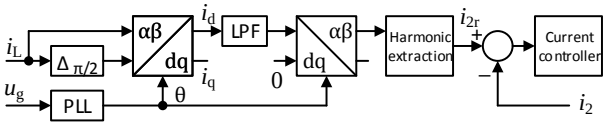

Fig. 4: dq Control diagram

fundamental harmonic reactive component. Fig. 4 shows a control diagram in the dq frame, with compensation of the higher harmonics and the fundamental harmonic reactive component. In the harmonic extraction block, the load current fundamental harmonic signal is subtracted from the load current signal i_L. The difference between these current signals is the harmonic current signal i_h and forms the reference for the current control loop. The current controller is a linear controller of the PI type. In dq frame a single-phase system can be translated directly into an α-β frame without matrix conversions by shifting β by 90° relative to α (i_L). To generate the fundamental harmonic, the active component (i_d) and the θ obtained from the PLL are needed [7]. After the generation of the α from the i_d, the rest of the control proceeds to harmonic extraction block previously described (Fig. 3).

III. Systems simulations

A. Simulations on nonlinear load

This subsection shows the responses of current harmonics filtering in a circuit with a nonlinear load "Load 1" (Fig. 2). Reason for choosing RL was the simplicity of its realisation in a laboratory environment to test the prototype active filter. Two cases have been considered. The converter side current i_1 and the grid side current i_2 (Fig. 1) are used as feedback signals.

Fig. 5 represents the first case, showing the waveform of the load current (blue), the active filter current (red) and the grid current (green). The load current RMS value is 15.35 A and the grid current RMS is 14.0 A. The load current *THD* is 42.3%, and the grid current *THD* after filtering is 2.76% (Fig. 6).

Fig. 7 shows the load, filter and grid current waveforms for the case where the current i_2 is used as feedback signal. The RMS value of the load current is 15.35 A and the grid current RMS is 14.1 A. The load current *THD* is 42.3%, and the grid current *THD* after filtering is 1.55%. With the same setting of the PI controller, the grid current *THD* is lower when current i_2 (Fig. 8) is used as feedback signal than when current i_1 (Fig. 6) is used as feedback signal.

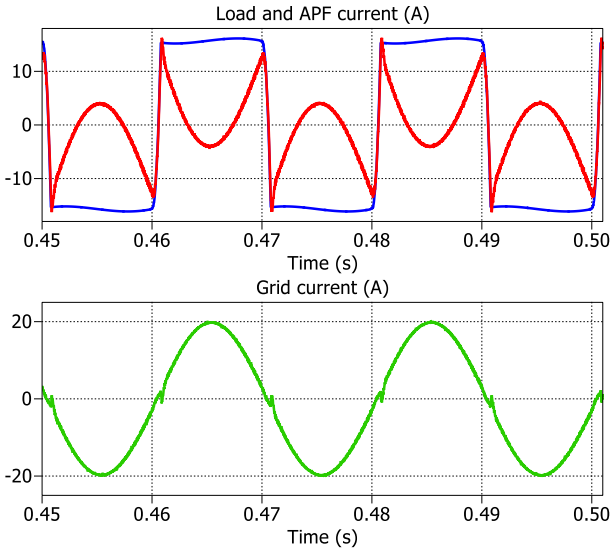

Fig. 5: Current waveforms using converter side current (i_1) as a feedback signal

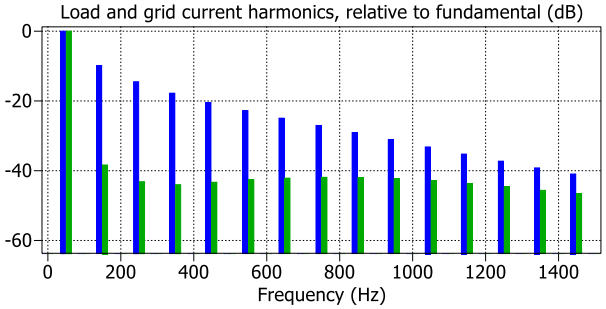

Fig. 6: Current harmonics spectrum using converter side current (i_1) as a feedback signal

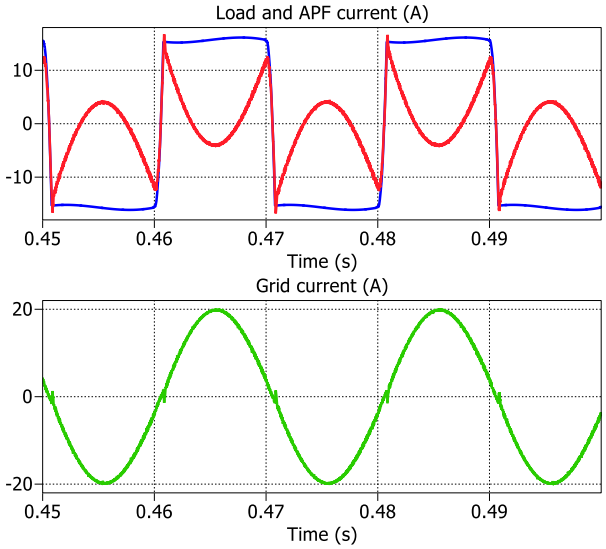

Fig. 7: Current waveforms using grid side current (i_2) as a feedback signal

For simulations in dq frame presented below, the current i_2 was used as feedback signal (Fig. 9).

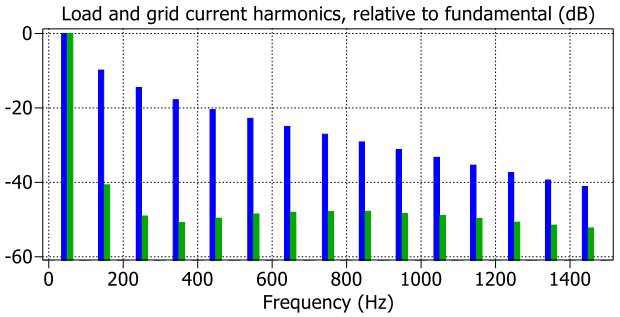

Fig. 8: Current harmonics spectrum using grid side current (i_2) as a feedback signal

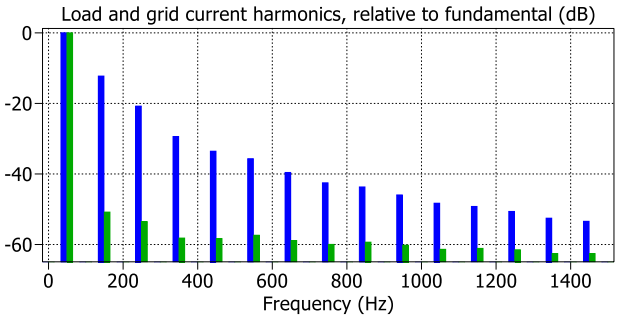

Fig. 10: Current harmonics spectrum using dq frame control and grid side current (i_2) as a feedback signal

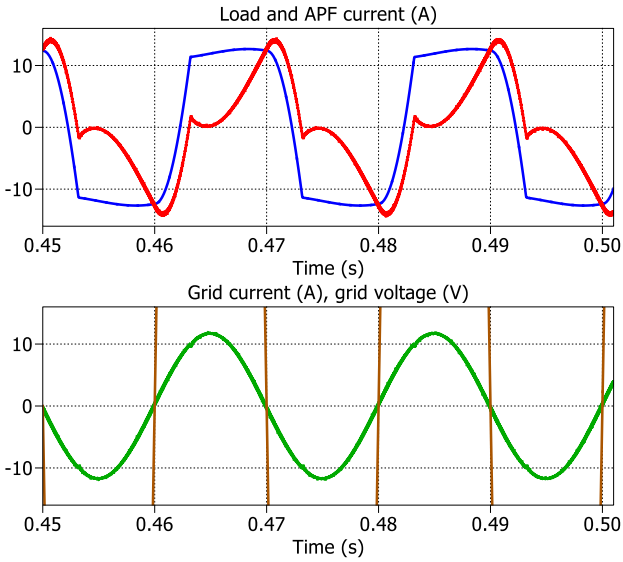

Fig. 9: Current waveforms using dq frame control and grid side current (i_2) as a feedback signal

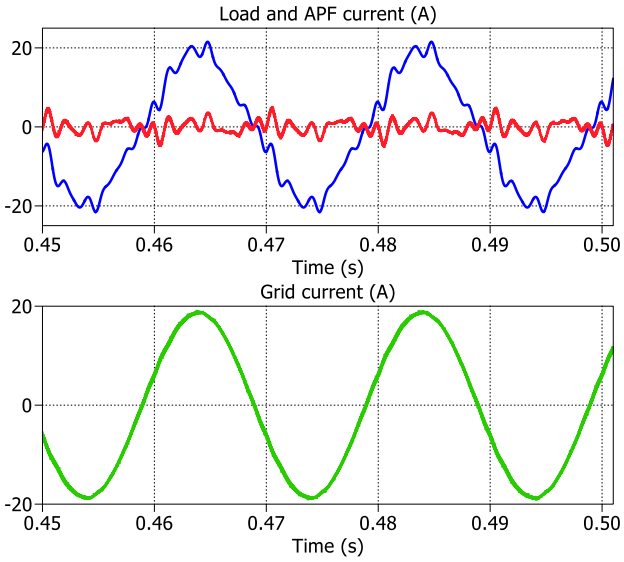

Fig. 11: Current waveforms using measured data rack harmonics as load current

In order to compensate for the fundamental current harmonic reactive component, a control is carried out in the dq frame. The inductance L_s value was increased from $1mH$ to $20mH$. The load current *THD* was decreased from 42.3% to 26.5%, due to the inductance L_s higher value. The load current waveform has a lower slope and a lower *THD*. The load current harmonics from the 15th harmonic upwards are smaller than -40 dB, whereas in the case with $1mH$ only the 29 harmonic is smaller than -40 dB. The grid current *THD* is 0.5% (Fig. 10), whereas in the first case it is 1.55%.

B. Simulations with measured load current harmonics

Fig. 11 and Fig. 12 show the load, APF and grid current waveforms as well as the harmonic spectrum for the case where the load was simulated with real current harmonics data measured in the data center. These measurements were made in data center rack with data servers. The load current RMS value is 13.34 A and the grid current RMS is 13.25 A. The load current *THD* is 11.94%, and the grid current *THD* after filtering is 0.66%.

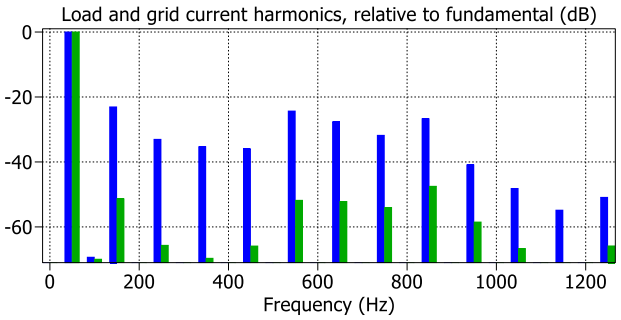

Fig. 12: Current harmonics spectrum using measured data rack harmonics as load current

Measurements on another rack with communication equipment show a higher current distortion (Fig. 13, blue). Since the equipment is underloaded, the load current *THD* is 47% with an RMS value of 1.82A. After filtering, the grid current *THD* is 2.11% and the RMS value of 1.56A (Fig. 14).

The case with real load current harmonics data from the data center was also simulated in the dq frame. The

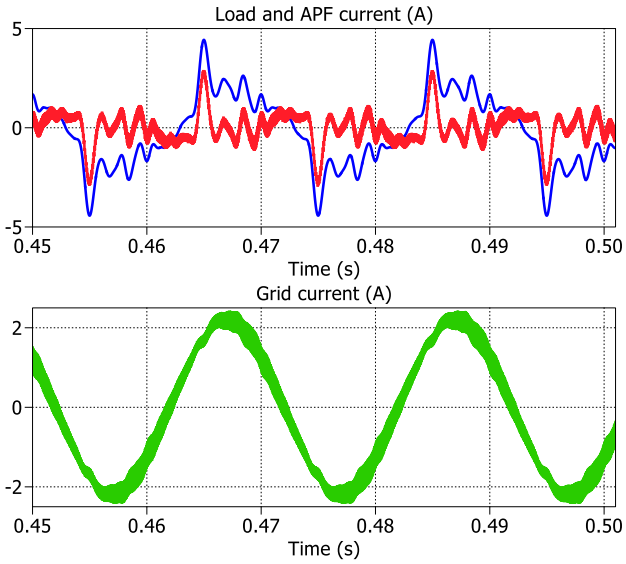

Fig. 13: Current waveforms using measured comunication rack harmonics as load current

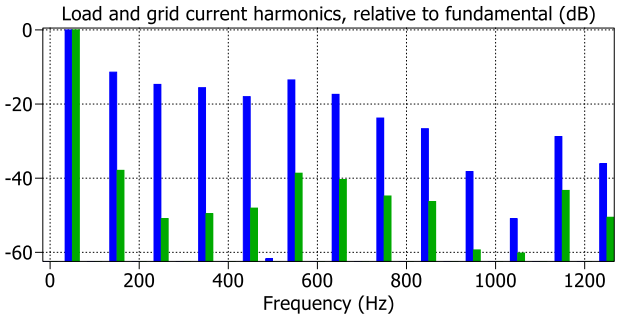

Fig. 14: Current harmonics spectrum using measured comunication rack harmonics as load current

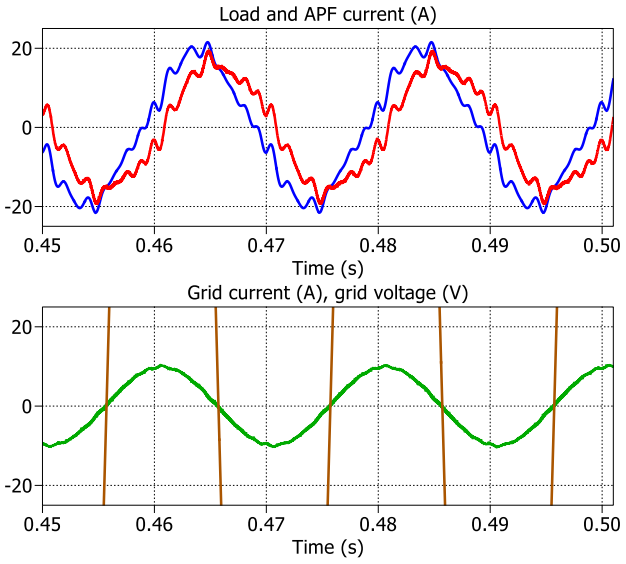

Fig. 15: Current waveforms using dq frame control and measured data rack harmonics as load current

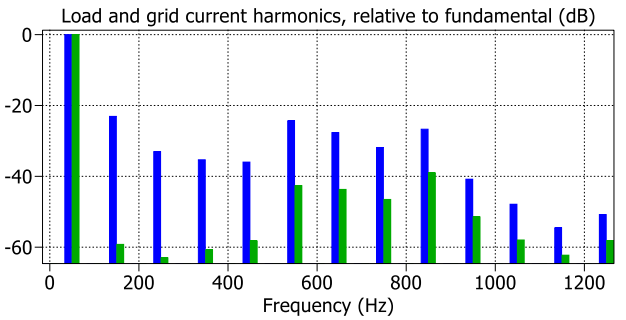

Fig. 16: Current harmonics spectrum using dq frame control and measured data rack harmonics as load current

load current fundamental harmonic lags the grid voltage by 60°. The load current RMS value is 13.34 A and the grid current RMS is 7.04 A (Fig. 15). The load current *THD* is 11.94%, and the grid current *THD* after filtering is 1.61% (Fig. 16).

IV. CONCLUSION

The paper presents two Shunt Active Power Filter simulations. The first simulation refers to a filter used only to reduce the current harmonics, while the second simulation uses a filter that also acts on the current reactive component. In the first simulation, the grid side and converter side currents were used as the current feedback signal. With the same settings of the PI controller, the grid current *THD* is lower when the grid side current is used as the feedback signal. For this reason, only the grid side current was used as the current feedback signal in the second simulation with control in the dq frame. Two types of loads were considered, an RL load and a load represented as a current source with current harmonic values measured in the data center. In both cases, the current *THD* after filtering is reduced to a value of less than one tenth of the original value. Future work will be based on experimental verification of the Shunt Active Power Filter prototype.

REFERENCES

[1] L. Zhou, Z. Liu, Y. Ji, D. Ma, J. Wang, and L. Li, "A improved parameter design method of lcl apf interface filter," in *2020 IEEE International Conference on Artificial Intelligence and Computer Applications (ICAICA)*, 2020, pp. 948–952.

[2] H. Yuan and X. Jiang, "A simple active damping method for active power filters," in *2016 IEEE Applied Power Electronics Conference and Exposition (APEC)*, 2016, pp. 907–912.

[3] C. Xie, Z. Wang, and G. Chen, "A simple method of realization of low power loss and high compensation-precision active power filter," in *2009 International Conference on Sustainable Power Generation and Supply*, 2009, pp. 1–5.

[4] M. Büyük, A. Tan, K. Ç. Bayindir, and M. Tümay, "Analysis and comparison of passive damping methods for shunt active power filter with output lcl filter," in *2015 Intl Aegean Conference on Electrical Machines & Power Electronics (ACEMP), 2015 Intl Conference on Optimization of Electrical & Electronic Equipment (OPTIM) & 2015 Intl Symposium on Advanced Electromechanical Motion Systems (ELECTROMOTION)*. IEEE, 2015, pp. 434–440.

[5] Y. Zhang, Z. Dai, and Y. Fang, "Voltage feed forward shunt active power filter based on double loop control," in *2021 International Conference on Power System Technology (POWERCON)*, 2021, pp. 1251–1256.

[6] W. Zhao, Y. Li, and G. Chen, "A double-loop current control strategy for shunt active power filter with lcl filter," in *2009 IEEE International Symposium on Industrial Electronics*, 2009, pp. 1841–1845.

[7] V. Khadkikar, M. Singh, A. Chandra, and B. Singh, "Implementation of single-phase synchronous d-q reference frame controller for shunt active filter under distorted voltage condition," in *2010 Joint International Conference on Power Electronics, Drives and Energy Systems, 2010 Power India*, 2010, pp. 1–6.